TECHNICAL TRANSACTIONS 4/2017
CZASOPISMO TECHNICZNE 4/2017
MECHANICS
DOI: 10.4467/2353737XCT.17.061.6372

Marian Sikora (marian.sikora@bwigroup.com)
BWI Poland Technologies sp. z o. o., Kraków

The pressure and the vibration measurement in automotive shock absorbers

Pomiary drgań i ciśnienia w amortyzatorze hydraulicznym w zawieszeniu samochodowym

Abstract

The purpose of this article was to develop a measurement system for analyzing the dynamic behavior of automotive hydraulic dampers as well as to examine the internal pressures in each hydraulic chamber of the damper. Dampers are one of the components of the vibration/noise system that originates at the contact point/surface between the wheel and the road, and then ends at the body of the vehicle. Specifically, dampers are often a source of flow-induced or motion-induced noise due to the operation of the valves. In this paper, measurement results are presented in the form of time histories of the internal pressures and piston rod acceleration, respectively. Fast Fourier Transform (FFT) graphs are also presented in order to identify the major components of the phenomena under investigation in a frequency domain.

Keywords: automotive, double-tube shock absorber, vibration, noise, dynamics

Streszczenie

Celem poniższego artykułu jest stworzenie systemu pomiarowego umożliwiającego badanie dynamiki pracy amortyzatora hydraulicznego oraz pomiar zmian ciśnienia w jego komorach roboczych. Amortyzator hydrauliczny jest istotną częścią układu zawieszenia pośredniczącą między drogą i kołem a karoserią samochodu. Wraz z elementami mocującymi i sprężyną zawieszenia stanowi ścieżkę przekazywania siły na samochód od podłoża. Amortyzatory hydrauliczne są często źródłem hałasu spowodowanego przepływem cieczy lub pracą zaworów hydraulicznych. W celu lepszego zrozumienia zjawisk zachodzących w obiekcie w artykule zostały umieszczone przebiegi czasowe obserwowanych wielkości fizycznych. Analiza częstotliwościowa (FFT) pozwoliła na wskazanie charakterystycznych częstotliwości drgań w amortyzatorze.

Słowa kluczowe: przemysł samochodowy, amortyzator hydrauliczny dwururowy, drgania, hałas, dynamika

1. Introduction

In brief, the automotive vehicle suspension shock absorber or a damper has been a well-known and established technology in the industry [2]. Its success has been due to its simplicity and modular design. Lessons learned over the years allowed for the elimination of assembly problems and specialized production. At the same time, from the engineering standpoint, a typical passive vehicle damper is a compromise between handling properties of a car, passenger comfort and safety as well as NVH (Noise, Vibration, and Harshness). Despite its simplicity, a good damper design is always an engineering challenge. Recently, new automotive trends in vehicle chassis design have generated new research and engineering efforts. For example, the engine and powertrain noise reduction have caused all noise sources due to vehicle chassis operation to become recognizable and audible by both the driver as well as the passengers. It is, therefore, vital to propose means for eliminating and/or improving the passenger comfort through changes in the device that would result in noise reduction.

The force output of vehicle dampers is a sophisticated function of the hydraulic valve's characteristics, damper geometry, compliance of fluid chambers, cavitation, friction, gas pressure, fluid properties, etc. In general, the subject of damping force generation in the automotive damper has been under consideration for years. Lang [10] developed a dynamic model of a twin-tube damper. The author considered the contribution of oil compressibility along with cylinder wall expansion and vapor generation. The model of a preloaded spring type valve included the disc inertia as well as viscous damping forces, contact force, geometric preload and force due to change in momentum of the fluid. By far, the work of Lang has remained the most cited academic contribution to the topic of damping force generation in the devices. Further efforts to model the damping force output of this device are well known Duym [3, p. 109–127], Farjoud [6, p. 1437–1456], Ferdek [7, p. 627–638]). On the NVH side, Kruse [8, 9] highlighted three basic approaches towards noise reduction. Optimizing the damping force allows one to reduce force excitation. It could lead to damper performance deterioration. Optimizing the damper mount reduces the noise transmission. Often it is a sufficient method; however, it does not change the basic phenomena. According to Kruse, the optimum way to meet customer requirements was to modify the dynamic structural properties for the reduction of vibrational response. In his study, the author included the measurement of excitation displacement, damping forces, piston rod acceleration and pressures in fluid chambers of an exemplary damper. The modal analysis of piston rod dynamic behavior was also conducted. Finally, the displacement, damping force and acceleration measurements have formed an experimental base for the studies undertaken by Czop and Sławik [1, p. 1937–1955].

In the paper, the author reveals a measurement system for the acquisition of damper internal phenomena. The test approach includes the measurements of piston rod acceleration, displacement and internal pressures. The test configuration allows the investigation of phenomena occurring in the damper under various operating conditions. In the paper, the author presents several data sets performed at a number of excitation frequencies and the peak velocity of 0.25 m/s. In-depth analysis of the obtained results is also performed in detail.

2. Measurement system

In this section, the author highlights all key elements of the damper measurement system. Some approach examples can be find in papers [4, p. 39–47], [5, p. 24–29]. To conduct the measurement, the MTS hydraulic actuator was used as shown in Fig. 1. As shown, the damper's reservoir was rigidly attached to the MTS's fixture subjected to sinusoidal displacement inputs. The damper piston rod was then attached to the elastic (rubber-type) top mount (the top mount stiffness is maintained at the same level during all experiments). The top mount is connected to the upper head of the MTS hydraulic actuator. In this configuration, the damper can be operated in a manner similar to that in a real vehicle.

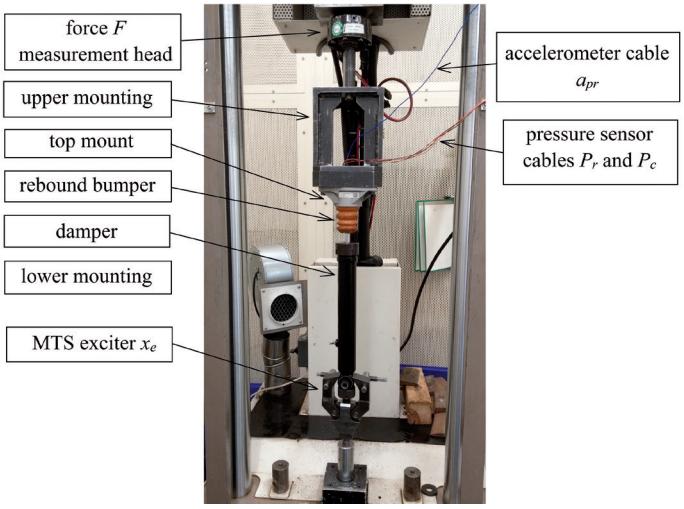

Fig. 1. Measurement test rig

The base parameters of the investigated damper configuration were: piston rod mass – 0,4 kg, gas pressure: 6 bar; maximum length in extension: 540 mm; maximum displacement (stroke): 150 mm; inner tube diameter: 32 mm; piston rod diameter: 14 mm; inlet cross-section area (rebound): 25 mm^2; inlet cross-section (compression side): 22,7 mm^2.

The LMS AD/DA card SCADAS III is used in the measurement system for the purpose of data acquisition and PC communication. Acceleration and pressure signals are then directly registered by the LMS module. The displacement and force signals are collected by the MTS controller, and then transferred to the LMS card at the sampling rate of 12.8 kHz.

During the tests, the damper was subjected to oscillatory sinusoidal displacement inputs at the peak velocity of 0.25 m/s as follows:

- +/–30 mm 1.33 Hz;
- +/–8 mm 5 Hz;
- +/–4 mm 10 Hz;
- +/–2 mm 20 Hz.

The experimental damper prototype was instrumented in such a way to fit two pressure sensors PA-4LC for acquiring the pressure signals in rebound and compression fluid chambers, respectively. As shown in Fig. 3, the respective pressure signals were then collected using the sensors in the P&R (piston and rod) assembly, located above and below the piston. Technical specifications of the PA-4LC sensors are:

Table 1. Pressure sensor – parameters [11]

Type	Dimensions [mm]	**Pressure Range**	**Storage Temperature**	**Operating Temperature**	**Output**
4 LC	Ø11 × 4.2	0 … 100 bar abs.	–10 … +80°C	0 … 50°C	0.5 … 4.5 V

The goal of the bench test was not to reproduce exact on-the-vehicle test conditions, but to conduct comparison analysis. Although the top mount of a damper has a big influence on the acceleration level on the car, the measurement still gives useful data. It allow to test different configurations of the damper in a simple way on a component level.

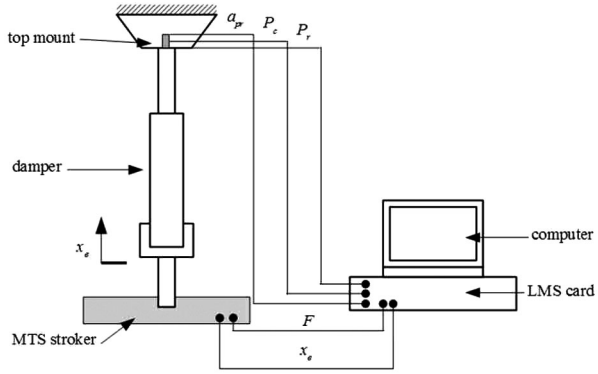

Fig. 2. Measurement system layout. Measured signals: excitation displacement – x_e, piston rod acceleration – a_{pr}, pressure in compression chamber – P_c, pressure in rebound chamber – P_r and damping force – F

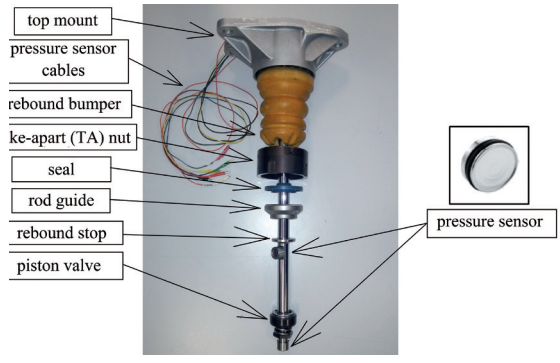

Fig. 3. Instrumented piston rod and top mount unit incl. 4 LC type pressure sensors [11]

3. Measurements results

The results of measurements are presented in the form of time histories of pressures, displacements and acceleration. The prescribed tube displacement input was measured during the experiment. The measured output was piston rod acceleration (not displacement). Moreover, pressure difference vs. excitation displacement and excitation velocity is presented, too. The results are illustrated in Figs. from 4 to 9.

Charakterystyki siły nie zostały podane w funkcji przemieszczeń i prędkości względnych ponieważ w układzie nie jest mierzone przemieszczenie tłoczyska. Natomiast przemieszczenie uzyskane drogą całkowania jest obarczone szeregiem błędów całkowania oraz nieznajomością warunków początkowych.

The high amplitude and low frequency excitation (see Fig. 4) show a low dynamic state. Both movements are separated. During the rebound (upward) movement, the pressure in the rebound chamber is around 2.4 MPa, the pressure in the compression chamber is low, slightly decreasing down to gas pressure. During the compression (downward) movement, the pressure in the rebound chamber is around 3.45 MPa and the pressure in the compression chamber is 4.15 MPa. At transition points, the pressures in both chambers are low and close to gas pressure.

As the frequency of the excitation increases, the situation changes. Figs 5a, 6a and 7a show that the maximum acceleration amplitude increases with the excitation frequency. The biggest change can be observed at the rebound-compression transition point. In the dynamic situation, the pressure in the rebound chamber is not fully released (see Fig. 5b, Fig. 6b and Fig. 7b). The pressure drop vs. displacement plots (see Fig. 5c, Fig. 6c and Fig. 7c) and pressure drop vs. velocity graphs (see Fig. 5d, Fig. 6d and Fig. 7d) show that the damping efficiency decreases with the excitation frequency (on the component level).

The low amplitude and high frequency (Fig. 7) show the dynamic situation in detail. During the rebound movement, the pressure level in the rebound chamber is approx. 2.3 MPa, the pressure in the compression chamber is low and slightly decreasing to the gas pressure level. While during the compression, the pressure in the rebound chamber is much lower at approx. 1.87 MPa, and the pressure in the compression chamber is 2.35 MPa. The pressure signal is shifted with respect to the displacement excitation input. During the transition (rebound-compression), the pressures in both chambers are still low and close to the gas pressure level. For comparison, during the compression-rebound transition, the damper operation is delayed. Effectively, the rebound pressure is not relieved and maintained at a relatively high amplitude of the internal pressure.

Fig. 8 shows the FFT of the rod acceleration signal calculated based on one cycle and normalized by the maximum input acceleration. Clearly, characteristic components appear around 360 Hz. The 20 Hz excitation results in frequency components augmented within the range of 260–500 Hz. Fig. 9 shows two configurations of the same damper assembly. The first one is basic, whereas the second one included modified valves (yet producing same steady-state force output). The modification allows to improve the dynamic characteristics; the dynamic force characteristics and controlled leaks were modified. The pressure in the compression chamber rises faster and achieves higher values. The pressure in the rebound chamber also shows bigger variance. At the compression-rebound transition, the second configuration shows a low-pressure fluctuation. As a result, a lower acceleration of the piston rod can be observed.

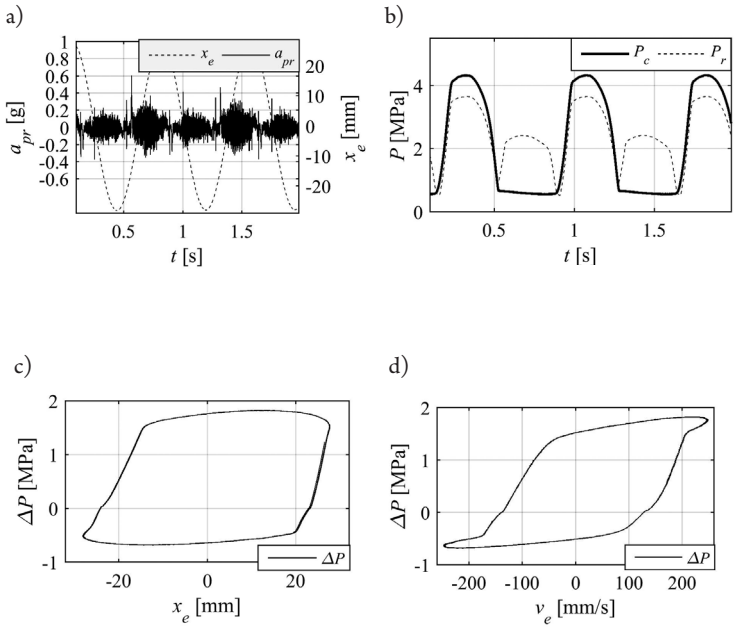

Fig. 4. Measurement results, excitation 1.33 Hz +/–30 m: a) piston rod acceleration a_{pr} and displacement x_e, b) pressure in compression P_c and rebound P_r chamber, c) pressure difference ΔP vs. displacement x_e, d) pressure difference ΔP vs. velocity v_e. ($\Delta P = P_r - P_c$)

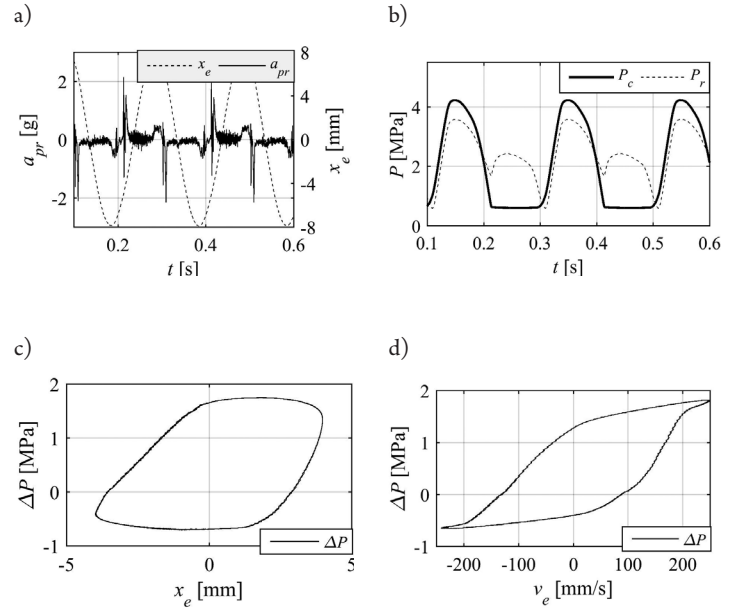

Fig. 5. Measurement results, excitation 5 Hz +/–8 mm: a) piston rod acceleration a_{pr} and displacement x_e, b) pressure in compression P_c and rebound P_r chamber, c) pressure difference ΔP vs. displacement x_e, d) pressure difference ΔP vs. velocity v_e. ($\Delta P = P_r - P_c$)

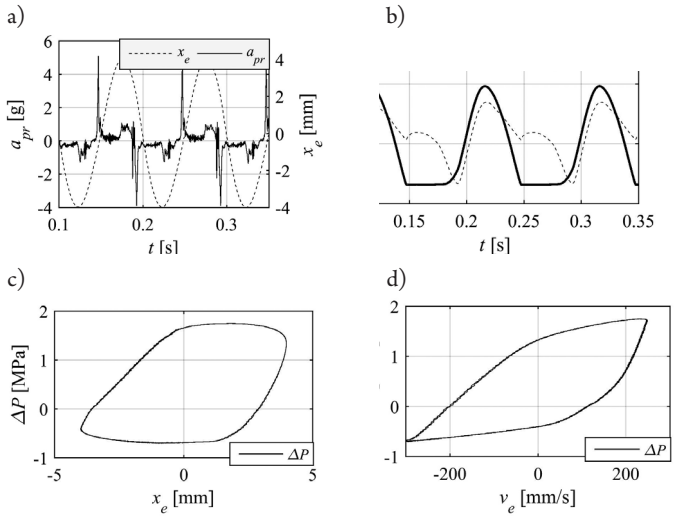

Fig. 6. Measurement results, excitation 10 Hz +/–4 mm: a) piston rod acceleration a_{pr} and displacement x_e, b) pressure in compression P_c and rebound P_r chamber, c) pressure difference ΔP vs. displacement x_e, d) pressure difference ΔP vs. velocity v_e ($\Delta P = P_r - P_c$)

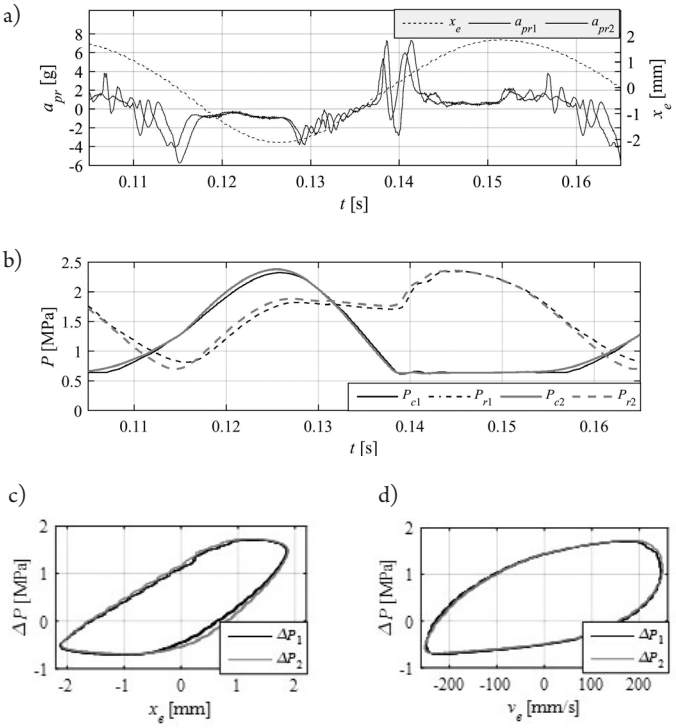

Fig. 7. Measurement results, excitation 20 Hz +/–2 mm: a) piston rod acceleration a_{pr1}, a_{pr2} and displacement x_e, b) pressure in compression P_{c1}, P_{c2} and rebound P_{r1}, P_{r2} chamber, c) pressure difference ΔP vs. displacement x_e, d) pressure difference ΔP ($\Delta P = P_r - P_c$) vs. velocity v_e. The subscript 1 refers to the first configuration, 2 denotes the second damper configuration

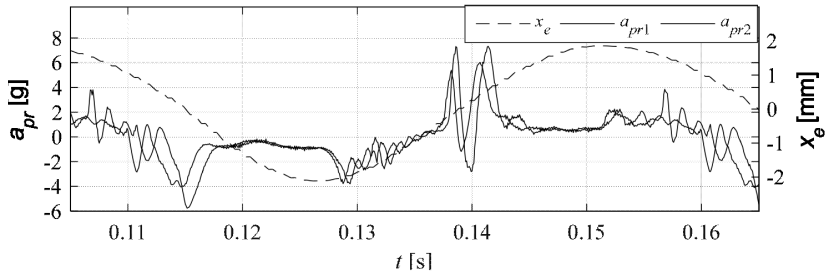

Fig. 8. The FFT of P&R acceleration, calculated based on one cycle and divided by maximum input acceleration (normalized to maximum input acceleration). Although input signal is a constant frequency sinewave (1.3 Hz; 10 Hz; 20 Hz), the output has a wide frequency band. The curves show the dynamic response of the system due to the internal phenomena

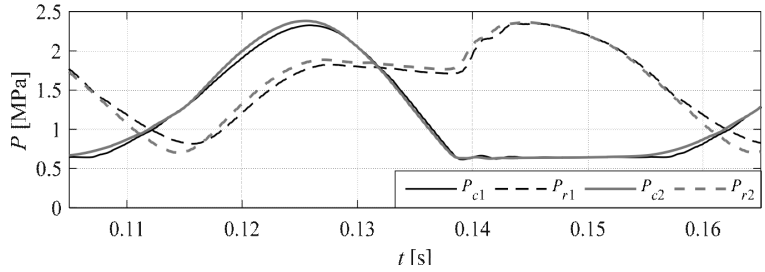

Fig. 9. The FFT of P&R acceleration, calculated based on one cycle and divided by maximum input acceleration (normalized to maximum input acceleration), dashed line present improved damper performance

4. Summary and conclusions

The proposed measurement test stand allows for the investigation of the dynamic characteristic of automotive double-tube shock absorbers. The developed instrumented prototype will be used for improving the dynamic behaviour of the valves in automotive dampers. In the paper, the author presents data acquired for the excitation frequencies up to 20 Hz, which is usually well above the natural frequency of unsprung mass in automotive vehicle suspensions. As the frequency of the excitation increased, the stroking amplitude decreased to maintain constant peak velocity. To conclude, the frequency has a direct impact on the operation of the examined valves. As the frequency increased, the rod acceleration was augmented, too. The acceleration peak amplitude was at the valve's transition points, i.e. at valve's opening/closing. The FFT analysis of the acceleration signal shows the natural frequency at approx. 360 Hz. It is, therefore, apparent that the flow-induced vibrations are transmitted through the top mount module to the body of the car. The phenomenon may be perceived as noise by passengers in the vehicle cabin.

Finally, further work will be focused on dynamic characterization of the damper under investigation, and a further improvement of the operation of the device.

References

[1] Czop P., Sawik D., *A high-frequency first-principle model of a shock absorber and servo-hydraulic tester*, Mechanical Systems and Signal Processing 25(6), August 2011, 1937–1955.

[2] Dixon J.C., *The shock absorber handbook*, Professional Engineering Publishing Ltd and John Wiley and Sons, 2007.

[3] Duym S., Steins R., Reybrouck K., *Evaluation of shock absorber models, Vehicle System Dynamics*: International Journal of Vehicle Mechanics and Mobility 27(2), 1997, 109–127.

[4] Dzierżek S., Knapczyk M., Malinowski M., *Extending passive dampers functionality for specific ride and handling requirements*, Czasopismo Techniczne, 6-M/2008, 39–47.

[5] Eickhoff M., Sonnenburg R., Stretz A., *Piston rod vibrations in damper modules – causes and remedies*, ATZ, Vol. 112, 2010, 24–29.

[6] Farjoud A., Ahmadian M., Craft M., Burke W., *Nonlinear modeling and experimental characterization of hydraulic dampers: effects of shim stack and orifice parameters on damper performance*, Nonlinear Dynamics, Vol. 67, Issue 2, January 2012, 1437–1456.

[7] Ferdek U., Łuczko J., *Modeling and analysis of a twin-tube hydraulic shock absorber*, Czasopismo Techniczne, 2-M/2012, 627–638.

[8] Kruse A., *Analysis of dynamic pressure build-up in twin-tube vehicle shock absorbers with respect to vehicle acoustics*, SAE International, Vehicle Dynamics Expo 2008, Stuttgart 2008.

[9] Kruse A., *Characterizing and reducing structural noises of vehicle shock absorber system*, SAE Technical Report 2002-01-1234, 2002.

[10] Lang H.H., *A study of the characteristics of automotive hydraulic dampers at high stroking frequencies*, The University of Michigan, 1977.

[11] Pressure sensor data sheet: http://www.keller-druck.com/picts/pdf/engl/4lc_9lc_e.pdf (access: 14.04.2015).